Robust Optimization and Uncertainty Quantification of a Permanent Magnet Synchronous Motor's Geometry

Oliver Lass[1], Stefan Ulbrich[1], Zeger Bontinck[2,3], Herbert De Gersem[3], Sebastian Schöps[2,3]

[1]Chair of Nonlinear Optimization, Department of Mathematics, Technische Universität Darmstadt, Germany
[2]Graduate School of Computational Engineering, Technische Universität Darmstadt, Germany
[3]Institut für Theorie Elektromagnetischer Felder, Technische Universität Darmstadt, Germany

The volume and position of permanent magnet material in a synchronous machine are optimized. The paper proposes a *robust* optimization process which also accounts for geometric uncertainties. The results are also verified by stochastic collocation and show a slightly worse optimum, which is however robust against manufacturing tolerances.

***Index Terms*—Finite element analysis, optimization, permanent magnet machines, robustness.**

I. Introduction

The price of permanent magnet (PM) material motivates optimization of PM synchronous machine (PMSM) designs. Standard optimization procedures bring improvements but partially sacrifice the robustness of the original design e.g. with respect to manufacturing tolerances. This may cause the promised improvements to become unrealistic and thus irrelevant. This paper accounts for such uncertainties during the optimization process in order to come up with a *robust* optimized design.

In this paper a classical gradient-based optimization is used to improve the robustness of a known machine design. A large speed-up is obtained by using an affine decomposition of the geometry. The robustification is implemented by efficient evaluations of linear (or if necessary quadratic) approximations such that high numerical costs as e.g. in [1] are avoided. Finally the design is validated by using stochastic collocation [2].

II. Modeling and Discretization

The parameter $\mathbf{p} \in R^3$ is used to describe the location and size of the PMs within the rotor of the machine, where $\mathbf{p}_1$ is the width, $\mathbf{p}_2$ the height and $\mathbf{p}_3$ describes the central perpendicular distance between the PM and the surface of the rotor, see Fig. 1. The finite element (FE) approach leads to the system

$$\mathbf{K}(\mathbf{p})\mathbf{a}(\mathbf{p}) = \mathbf{j}_{\mathrm{src}}(\mathbf{p}) + \mathbf{j}_{\mathrm{pm}}(\mathbf{p}) \tag{1}$$

where $\mathbf{p}$ expresses the dependency of the FE system on the magnet's geometry and position within the machine's cross-section. To obtain a computationally fast model and to avoid remeshing, an affine decomposition is introduced. Therefore, a region around the PM (Fig. 1) is defined and decomposed into $L = 14$ triangles [3]. We can rewrite (1) as

$$\mathbf{K}(\mathbf{p}) = \mathbf{K}^{\mathrm{out}} + \sum_{k=1}^{L} \theta^k(\mathbf{p})\mathbf{K}^k, \tag{2}$$

where $\mathbf{K}^{\mathrm{out}}$ is the system matrix for the domain outside the box and $\mathbf{K}^k$ are the matrices corresponding to the triangular subdomains. The $\mathbf{p}$ dependency of the system is now only

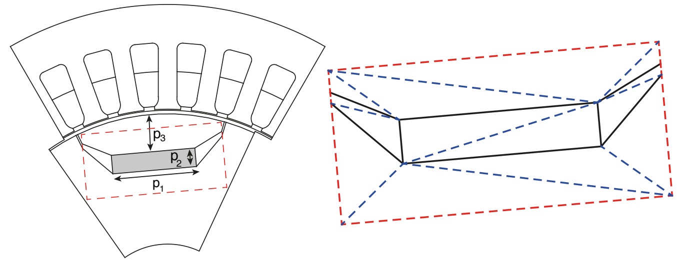

Fig. 1: Geometry of the model problem, region for the affine decomposition drawn with dashed lines.

present in the weight functions θ^k which are easy to evaluate. The same decomposition is performed for the right hand side.

Nonlinear material behavior was frozen during the optimization. However an extension is straightforward but might reduce the benefit of the affine transformation due to the necessity of reassembling some FE matrices $\mathbf{K}^k(\mathbf{a})$.

III. Optimization

The target of the optimization is to minimize the required PM material maintaining an effective value of the electromotive force (EMF) $\hat{\mathcal{E}} = 30.37\,\mathrm{V}$ at synchronous speed of 1000 rpm; other quantities, e.g., cogging torque could be considered similarly. The optimization problem under consideration is

$$\min_{\mathbf{p}\in R^3} J(\mathbf{p}) := \mathbf{p}_1\mathbf{p}_2 + \gamma \max(0, \hat{\mathcal{E}} - \mathcal{E}(\mathbf{p})), \tag{3}$$

where $\mathcal{E}(\mathbf{p})$ is the EMF for the configuration corresponding to $\mathbf{p}$ and $\gamma = 100$ mm^2/V is a weighting factor. Additionally we introduce the design constraints $\mathbf{p}_2 + \mathbf{p}_3 \leq 15\,\mathrm{mm}$ and $3\mathbf{p}_1 - 2\mathbf{p}_3 \leq 50\,\mathrm{mm}$ and the bounds for $(1\,\mathrm{mm}, 1\,\mathrm{mm}, 5\,\mathrm{mm}) \leq \mathbf{p} \leq (\infty, \infty, 14\,\mathrm{mm})$. Note that for the computation of the EMF, the solution of (1) is required. Hence, we have an optimization problem with a PDE constraint. The parameter $\mathbf{p}$ is uncertain due to the production process. Therefore, we introduce the robust counter part (worst-case) associated with (3) as

$$\min_{\mathbf{p}\,\in R^3} \max_{\delta\,\in U} J(\mathbf{p}+\delta), \quad \text{subject to} \quad \max_{\delta\,\in U} G(\mathbf{p}+\delta) \leq 0, \tag{4}$$

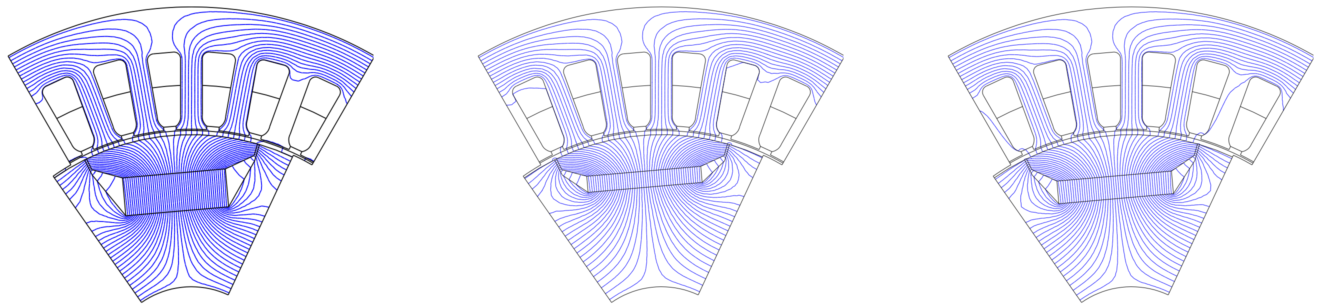

(a) Initial configuration:
$\mathbf{p} = (19.00\,\mathrm{mm}, 7.00\,\mathrm{mm}, 7.00\,\mathrm{mm})$,
Vol: $133\,\mathrm{mm}^2$; EMF: $30.37\,\mathrm{V}$.

(b) Configuration after optimization:
$\mathbf{p} = (21.07\,\mathrm{mm}, 2.98\,\mathrm{mm}, 6.61\,\mathrm{mm})$,
Vol: $62.80\,\mathrm{mm}^2$; EMF: $30.37\,\mathrm{V}$.

(c) Configuration after robust optimization:
$\mathbf{p} = (21.16\,\mathrm{mm}, 3.88\,\mathrm{mm}, 7.50\,\mathrm{mm})$,
Vol: $88.36\,\mathrm{mm}^2$; EMF: $31.40\,\mathrm{V}$.

Fig. 2: Magnetic flux lines in the obtained PMSM designs.

where $U := \{\delta \in R^3 \,|\, \|\delta\|_\infty \leq 0.3\,\mathrm{mm}\}$ is the uncertainty set and $G(\mathbf{p})$ is the collection of all the constraints previously introduced. To solve (4), the maximization problem can be approximated by linear or quadratic models [6] such that exact expressions can be inserted.

The cost functions in (3) and (4) are not smooth due to the $\max$ operator. For the optimization we seek a smooth formulation in order to apply derivative based methods. Therefore, the expression is equivalently expressed in terms of a slack variable ξ and the additional constraint $\hat{\mathcal{E}} - \mathcal{E}(\mathbf{p}) - \xi \leq 0$ is introduced. This optimization problem can then be solved by standard methods. The computation of the derivatives is performed using the sensitivity equations given by the derivatives of the weight functions $\theta^k(\mathbf{p})$. To perform the numerical optimization, a Sequential Quadratic Programming (SQP) method using damped BFGS updates as Hessian approximation is utilized. Combined with an Armijo backtracking strategy using a ℓ_1- penalty function, this method provides fast global convergence [4], [5].

Evolutionary algorithms were not considered since we aim for the improvement of an existing design and those algorithms require typically many model evaluations even when starting in the neighborhood of the optimal design. In a straight forward comparison the genetic algorithm took 45min (instead 2.37s for SQP) and 14h in the robustified case (instead of 5.37s).

IV. Numerical Results and Robustness

The results obtained by the optimization process are outlined in Fig. 2 and Table I. The volume of the PM can successfully be reduced while the prescribed EMF $\hat{\mathcal{E}} = 30.37\,\mathrm{V}$ is maintained. In the case of the robust optimization, also in the worst case (see Table II), the prescribed EMF $\hat{\mathcal{E}}$ is maintained, which underlines the advantage of the method. The computation times for the optimization procedures are $2\,\mathrm{s}$ and $4\,\mathrm{s}$, respectively. The results are verified by uncertainty quantification: the input uncertainty is propagated through the model by using stochastic quadrature [2]. A uniform distribution of δ on U is assumed, such that $\mathbf{p} = \mathbf{p}^{(i)} + \delta$ where $\mathbf{p}^{(i)}$ with $i \in \{\mathrm{a}, \mathrm{b}, \mathrm{c}\}$ corresponds to one of the three reference configurations; high-order Gaussian quadrature with 10^3 nodes was applied to compute the standard deviation of the EMF.

TABLE I: Comparison of the results obtained by the optimization procedures. The optimal parameter, the associated volume and the EMF are shown.

	Configuration	$\mathbf{p}$ (mm)	Vol (mm^2)	EMF (V)
(a)	Initial	$(19.00, 7.00, 7.00)$	133.00	30.37
(b)	Optimized	$(21.07, 2.98, 6.61)$	62.80	30.37
(c)	Robustified	$(21.16, 3.88, 7.50)$	88.36	31.40

TABLE II: Comparison of the deviations obtained by worst-case optimization and stochastic collocation.

	Configuration	Worst Dev. of EMF (V)	Std. Dev. of EMF (V)
(a)	Initial	0.80	0.30
(b)	Optimized	1.27	0.43
(c)	Robustified	1.04	0.36

V. Conclusion

The initial configuration has a poor performance but is robust. The traditionally optimized one is better but very sensitive and may even fail to achieve its nominal performance. The robust optimization yields an improved design.

Acknowledgment

This work is supported by the German BMBF in the context of the SIMUROM project, by the 'Excellence Initiative' of the German Federal and State Governments and the Graduate School of Computational Engineering at TU Darmstadt.

References

[1] Z. Ren, D. Zhang, and C.-S. Koh "An Improved Robust Optimization Algorithm: Second-Order Sensitivity Assisted Worst Case Optimization" *IEEE Trans. Magn.,* vol 49, pp. 2109 - 2112, 2013.

[2] D. Xiu, *Numerical Methods for Stochastic Computations: A Spectral Method Approach*, Princeton University Press, 2010.

[3] G. Rozza, D.B.P. Huynh, and A.T. Patera, "Reduced Basis Approximation and a Posteriori Error Estimation for Affinely Parametrized Elliptic Coercive Partial Differential Equations," *Arch. Comput. Methods. Eng.,* vol. 15, pp. 229-275, 2008.

[4] M. Hinze, R. Pinnau, M. Ulbrich, and S. Ulbrich, *Optimization with PDE Constraints. Mathematical Modelling: Theory and Applications, 23*, Springer Verlag, 2009.

[5] J. Nocedal, and S.J. Wright, *Numerical Optimization, second edition*, Springer Series in Operation Research, 2006.

[6] M. Diehl, H.G. Bock, and E. Kostina, "An approximation technique for robust nonlinear optimization," *Math. Program.,* Ser. B 107, pp. 213-230, 2006.